Dynamic impedance of two-dimensional superconducting films near the superconducting transition

Stefan J. Turneaure* and Thomas R. Lemberger
Department of Physics, Ohio State University, Columbus, Ohio 43210-1106

John M. Graybeal†
Department of Physics, University of Florida, Gainesville, Florida 32611-8440
(Received 19 July 2000; published 3 April 2001)

The sheet impedances, $Z(\omega,T)$, of several superconducting a-$Mo_{77}Ge_{23}$ films and one In/InO_x film have been measured in zero field using a two-coil mutual inductance technique at frequencies from 100 Hz to 100 kHz. $Z(\omega,T)$ is found to have three contributions: the inductive superfluid, renormalized by nonvortex phase fluctuations; conventional vortex-antivortex pairs, whose contribution turns on very rapidly just below the Kosterlitz-Thouless-Berezinskii (KTB) unbinding temperature; and an anomalous contribution. The latter is predominantly resistive, persists well below the KTB temperature, and is weakly dependent on frequency down to remarkably low frequencies, at least 100 Hz. It increases with T as $e^{-U'(T)/k_BT}$, where the activation energy, $U'(T)$, is about half the energy to create a vortex-antivortex pair, indicating that the frequency dependence is that of individual excitations, rather than critical behavior.

DOI: 10.1103/PhysRevB.63.174505 PACS number(s): 74.25.Fy, 74.40.+k, 74.72.−h, 74.70.Ad

I. INTRODUCTION

For the past twenty years the superconducting to normal (S-N) transition in two-dimensional (2D) films and Josephson junction arrays has been a very active area of research, in the broad context of understanding the effects of reduced dimensionality on phase transitions. Interest has been revitalized by the quasi-two-dimensional nature of high-T_C cuprate superconductors. The paradigm for identifying and discussing the transition is the static Kosterlitz-Thouless-Berezinskii (KTB) theory,[1,2] and its extensions to dynamics,[3–5] which identify thermally excited vortex-antivortex pairs as the agents of dissipation and focus on them, setting aside nonvortex (longitudinal) phase fluctuations and fluctuations in the amplitude of the order parameter. Previous experimental studies have concentrated on power laws and critical scaling to test the validity of KTB theory in the narrow critical region.

In this paper, we present a comprehensive study of the sheet impedance of superconducting films in zero field, in which we pay particular attention to behavior below the critical region, in order to better understand the 2D S-N transition, and to establish a phenomenology for comparison with cuprates. Consistent with KTB, we find an abrupt increase in sheet inductance and a concurrent rapid increase in sheet resistance at the KTB transition temperature. But even well below this temperature there is an anomalous impedance, primarily resistive, that is not present in KTB theory. This impedance becomes apparent at low frequencies (below 100 kHz) where the inductive impedance of the superfluid is small. Its frequency dependence is weak, but extends to surprisingly low frequencies, down to at least 100 Hz. It is possible that the S-N transition actually occurs well below the KTB unbinding temperature, and is mediated by a more subtle, longer-lived, excitation than the classic vortex-antivortex pair.

Many previous studies of the S-N transition in 2D were scaling analyses of nonlinear dc current-voltage (I-V) characteristics,[6–10] and thus cannot be compared directly with our measurements. While these papers generally acknowledge good agreement with KTB theory, Pierson *et al.*[11] have revisited the scaling analyses of many I-V measurements, as well as dynamic measurements on 2D He films, and they find that when the dynamical exponent, z, is taken to be an adjustable parameter, the best scaling occurs for $z=5.6\pm0.3$, not the KTB value, $z=2$. Pierson *et al.* discount the notion that deviations of I-V curves from KTB at low current densities arise from finite-size effects, or vortices generated by the ambient field, or by vortex pinning, and conclude that the 2D S-N transition occurs below the universal KTB prediction, T_C. (A recent experimental and theoretical study of finite size effects in Josephson junction arrays can be found in Ref. 10.)

There have been several previous studies of dynamics of 2D superconductors, including indium-oxide[12] and a-MoGe films,[13] wire networks,[14] and Josephson junction arrays.[15,16] Where our data overlap these studies, there is good agreement. In particular, all studies find that at temperatures below the KTB unbinding temperature, the sheet impedance is frequency dependent at remarkably low frequencies. The present work expands on these studies.

The frequency dependence of the sheet impedance provided by vortex-antivortex pairs has been explored theoretically in some detail. Ambegaokar and co-workers extended the static KTB theory in the context of vortex-antivortex dynamics in superfluid He films.[3] Halperin and Nelson extended this work to vortex-antivortex pairs in superconducting films.[4] Minnhagen[5] pointed out that Ambegaokar's expressions for the sheet conductivity violate the Kramers-Kronig relationship, and he has developed a model similar to that of Ambegaokar that remedies this problem. The Minnhagen phenomenology (MP) provides an expression for the vortex dielectric function, which determines the imaginary conductivity contributed by vortex antivortex pairs. The real conductivity is determined by Kramers-Kronig transform.

The present work explores in detail the frequency and

temperature dependence of the sheet impedance, $Z(\omega,T)$, of a model 2D superconductor, amorphous MoGe, at normal-state sheet resistances R_N up to 900 Ω, and, for comparison, an amorphous-composite In/InO_x film with R_N near 4000 Ω. That these rather different materials share the same qualitative features indicates that the anomalous sheet impedance is general, not peculiar to a particular system. It follows that there exists an anomalous fluctuation that dominates the low-frequency behavior of Z below T_C, defined experimentally as the temperature where the sheet resistance and inductance increase very rapidly, consistent with vortex pair unbinding. This fluctuation must involve phase slips, hence vortices of some configuration. In Sec. IV we show that the conventional understanding of vortex-antivortex pairs does not capture their dynamics.

Before examining the data, it is useful to recall some of the principles and notations surrounding fluctuation effects. Thermal fluctuations become important in 2D superconductors, (films and Josephson junction arrays), when k_BT becomes comparable to the mean-field superconducting energy, U_{00}:

$$U_{00}(T) \equiv (\phi_0/2\pi)^2 L_0^{-1}(T), \tag{1}$$

where $\phi_0 \equiv h/2e$ is the flux quantum. The mean-field inverse sheet inductance, $L_0^{-1}(T)$, in Eq. (1) is proportional to the mean-field areal superfluid density, $n_{S0}(T)$, and it vanishes at the mean-field transition temperature, T_{C0}. $U_{00}(0)$ is typically one or two orders of magnitude larger than k_BT_{C0}, so thermal fluctuations become important very near T_{C0}, where $n_{S0}(T)$ is one or two orders of magnitude smaller than $n_{S0}(0)$. In 2D films, thickness $d \ll \xi(T)$, where $\xi(T)$ is the Ginzburg-Landau (GL) coherence length, $U_{00}(T)$ is the mean-field condensation energy, $V_C[B_C^2(T)/2\mu_0]$, in a coherence volume, $V_C \equiv 4\xi^2(T)d$. One can also write: $U_{00} = \hbar^2 n_{S0}(T)/4m$, where m is the electron mass, to make explicit the relationship between U_{00} and superfluid density. In square Josephson junction (JJ) arrays, U_{00} is the mean-field Josephson coupling energy, J, of one junction; for triangular and honeycomb arrays, U_{00} differs from J by a geometric factor near unity.[17] When U_{00} is written in terms of sheet inductance, as in Eq. (1), the expression is the same for films and arrays.

For our films, $U_{00}(T)$ can be obtained by extrapolation of low temperature data using the weak coupling BCS result for $n_{S0}(T)/n_{S0}(0)$. A more useful energy, $U_0(T)$, can be obtained from Eq. (1) by using the inductance of the background superfluid in place of the mean-field inductance. The background superfluid density, which is lower than the mean-field superfluid density due to the presence of nonvortex fluctuations, cannot be measured directly. However, since the contribution of vortex-antivortex pairs is small except very close to the unbinding temperature, below the critical region it is sufficient to calculate $U_0(T)$ using the measured sheet inductance, exclusive of the anomalous part. In the critical region, U_0 is estimated to be about 25% smaller than U_{00}, based on numerical simulations of Josephson junction arrays[17] and measurements on MoGe films.[18]

Regardless of details, one would expect the S-N transition to occur near $k_BT/U_{00}(T) = 1$. The full KTB renormalization group theory predicts the S-N transition at $k_BT/U(T) = \pi/2$, where the superconducting energy, $U(T)$, is calculated via Eq. (1) but with the effective sheet inductance, $L(T)$, including vortex-antivortex pairs, in place of the mean-field inductance. Numerical simulations of square, triangular, and honeycomb JJ arrays[17] find that L_0/L is about 0.6 at the KTB transition temperature, so that the transition occurs at $k_BT_C/U_{00}(T_C) \approx 0.9$. Consistent with this, we have found that the inverse sheet inductance of the a-MoGe films discussed below drops precipitously at $k_BT/U_{00}(T) \approx 0.9$, when the anomalous component of the sheet impedance is set aside.[18] Furthermore, fluctuations suppress the inverse sheet inductance to about 60% of its mean-field value just before the rapid drop. On this basis, we argue that the impedance of our films should be interpreted as the expected impedance of superfluid plus vortex pairs, plus an anomalous contribution.

It is straightforward to identify the anomalous impedance, $Z_a(\omega,T)$. Below T_C, as discussed below, vortex-antivortex pairs should be inductive at our experimental frequencies, so all of the sheet resistance, $R(\omega,T)$, is anomalous. The anomalous part, $L_a(\omega,T)$, of the experimental sheet inductance, $L(\omega,T)$, can be identified from its dependence on ω, since the inductance of the background superfluid plus bound vortex-antivortex pairs, $L_{SF}(T)$, is independent of frequency at temperatures and frequencies of interest here. Theories focus on the sheet conductance, $G(\omega,T) = \sigma_1(\omega,T)d - i\sigma_2(\omega,T)d \equiv Z^{-1}(\omega,T)$, especially the peak in $G_1(\omega,T)$ vs T, so we present our data in this form, too. But in our view, at temperatures below the very narrow critical region below T_C, the impedance, $Z(\omega,T)$ is more transparent because the impedances of the superfluid background and thermal vortex pair excitations are in series, in analogy with the impedance of pinned vortices.[19]

The outline of this paper is as follows. In Sec. II, the experimental method and sample properties are discussed. In Sec. III, experimental results are presented and features common to all films are highlighted. Section IV outlines conventional properties of individual vortex-antivortex pairs and then argues that unbinding of conventional pairs is responsible for the rapid changes in Z at and above the experimental T_C, but cannot account for the anomalous impedance below T_C. Section V summarizes our results for the anomalous impedance and shows how they compare to data in the literature.

II. EXPERIMENTAL METHOD AND SAMPLE PROPERTIES

The sheet impedance, $Z(\omega,T)$, was determined at frequencies, $f = \omega/2\pi$, from 100 Hz to 100 kHz using a two-coil mutual inductance technique with the drive and pickup coils coaxial and pressed against opposite sides of the film.[20] The drive coil radius is much smaller than the film dimensions, so the magnetic field it produces is concentrated near the center of the film. By means of a lookup table containing over 10 000 pairs of mutual inductance, M, and Z values, calculated for the geometry of the actual film and coils, the real and imaginary parts of Z were determined from the in-

TABLE I. Film parameters, Films *B, C, F,* and *G* are amorphous a-$Mo_{77}Ge_{23}$, and film *I* is amorphous-composite In/InO_x. d is the nominal film thickness. $L^{-1}(0)$ is the measured inverse sheet inductance extrapolated to $T=0$ from $T=400$ mK. The normal state sheet resistance, $R_N(15\,\mathrm{K})$, is nominal for the MoGe films (Ref. 31) and measured for the In/InO_x film. The uncertainty in T_{C0} is about 15% of $T_{C0}-T_C$ for the MoGe films and somewhat larger for the In/InO_x film.

Film	*B*	*C*	*F*	*G*	*I*
d (Å)	61	46	27.5	21.5	190
$L^{-1}(0)$ $(\mathrm{nH})^{-1}$ (±4%)	13.29	9.55	4.21	2.57	0.692
R_N (Ω) (±5%)	287	387	674	885	4150
T_{C0} (K)5.559	5.043	3.881	3.167	3.048	
T_C (K) (±5 mK)	0.021	4.920	3.734	2.999	2.685
$(T_{C0}-T_C)/T_{C0}$ (±15%)		0.024	0.038	0.053	0.12

phase and quadrature components of *M*. Great care was taken to ensure that *Z* was independent of the excitation amplitude. Measurements also were performed as a function of perpendicular magnetic field to identify the field range over which *Z* was independent of field.[21] All data presented here were taken with the ambient field nulled sufficiently so as not to affect the film's impedance.

Table I lists film properties. 6 mm radius a-$Mo_{77}Ge_{23}$ films with thicknesses down to 21.5 Å were grown on oxidized Si, with Ge buffer layers below and above. The beauty of these films is that, fluctuations aside, they are nearly perfect weak coupling BCS superconductors in the respect that, as shown in Refs. 18 and 21, their mean-field sheet inductances have the same BCS T dependence, that is, $L_0^{-1}(T/T_{C0})/L_0^{-1}(0)$ vs T/T_{C0} is the same for all, even though $L_0^{-1}(0)$ and T_{C0} vary substantially with thickness. Data also are presented for a 10 mm diameter In/InO_x film (film *I* in Table I). The superfluid density for this film does not follow the weak coupling BCS theory as well as MoGe films do, and in that sense it is less ideal.

III. EXPERIMENTAL RESULTS

In this section data are presented for the complex conductivity and impedance of several films. We emphasize that a great deal of effort went into ascertaining that data were taken in the linear response regime, where the sheet impedance was independent of the magnetic field produced by current in the drive coil, and into checking that the residual ambient field was negligibly small.[21]

A few comments about experimental uncertainties are in order. The experiment measures the magnetic field produced by induced currents in the sample. The current density does not vary through the thickness of our very thin films. Assuming that the film is homogeneous on a length scale much shorter than the 1 mm radii of the drive and pickup coils, the experiment yields $Z(\omega,T)$ directly. Uncertainty in the film thickness, *d*, enters only when we calculate the resistivity, $\rho \equiv Zd$. Signal-to-noise decreases as ω decreases because the measured pickup voltage is proportional to ω. Signal-to-noise decreases as T exceeds T_C and the field produced by currents in the sample becomes small. Uncertainty in R grows near the low temperature tail in σ_1. Here small uncertainties (less than 1°) in the phase of the mutual inductance are responsible. Since the dissipation peak extends to lower temperatures as ω is reduced, the sheet resistance is known with less accuracy for high frequencies at lower temperatures.

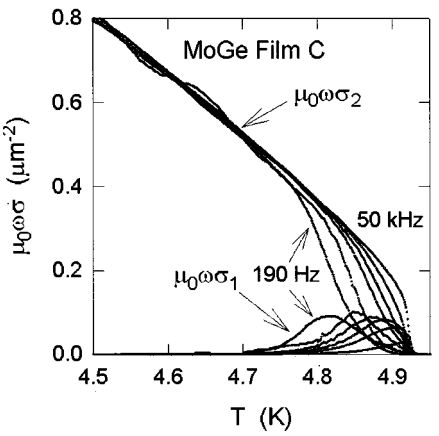

FIG. 1. T dependence of $\mu_0\omega\sigma$ for MoGe film *C* measured at $f=0.19$, 1, 2, 5, 10, and 50 kHz. $\mu_0\omega\sigma_2$ increases monotonically with frequency, and $\mu_0\omega\sigma_1$ peaks at higher temperatures as frequency is increased.

Figure 1 shows $\mu_0\omega\sigma$ vs T and Fig. 2 shows $L^{-1}(\omega,T)$ and $R(\omega,T)$ at $190\,\mathrm{Hz} \leqslant \omega/2\pi \leqslant 50\,\mathrm{kHz}$ for a-MoGe film *C*.

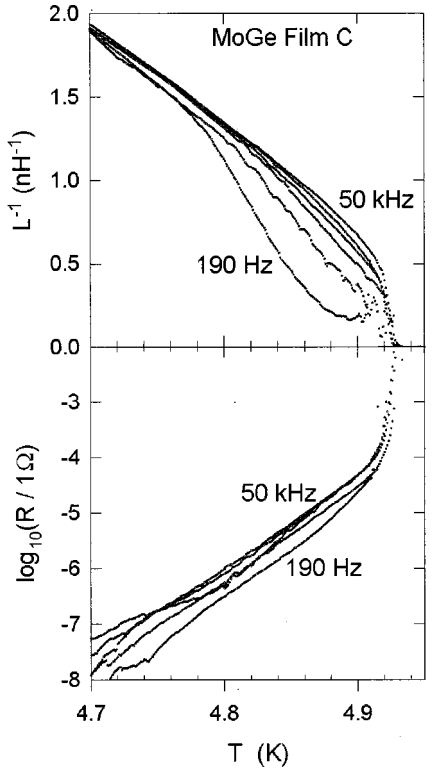

FIG. 2. T dependencies of L^{-1} and R for MoGe film *C*, calculated from data in Fig. 1.

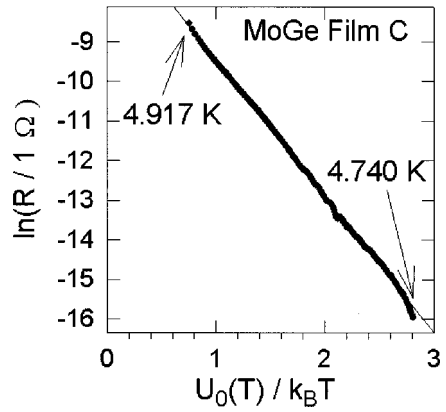

FIG. 3. ln(R) vs U_0/k_BT for film C at $f=50$ kHz. The linear fit indicates that $R(T)$ is Arrhenius with an activation energy of $3.5U_0$.

Consider data at 50 kHz. At about 4.92 K, R begins to increase very rapidly, and L^{-1} begins to drop. We define this temperature to be the experimental T_C, and we associate it with the unbinding of vortex-antivortex pairs. Below T_C, R is small, less than $10^{-6}R_N$, but it should be immeasurably small. Figure 3 shows that for $T<T_C$, R exhibits activated behavior with an activation energy of $3.5U_0(T)$, about half the energy needed to create a vortex-antivortex pair, as discussed below. It is possible that R vanishes at a phase transition well below T_C, but if so, the transition occurs when R is below our sensitivity. Finally, we note that R depends weakly on frequency down to 190 Hz, with no sign of saturation.

L^{-1} increases slowly with ω due to the frequency dependence of L_a. L_a can be extracted by fitting ωL with an ordinary inductive term, $\omega L_{SF}(T)$, which is strictly proportional to ω and includes the inductances of the superfluid and conventional vortex pairs, and an anomalous part, $\omega L_a(\omega,T)$, with a power law frequency dependence. It turns out that R and $\omega L_a(\omega,T)$ have the same power law dependence over several decades of frequency, and therefore are consistent with being Kramers-Kronig transforms of each other. This lends confidence to the separation of L into two components. Results for MoGe films *B*, *F*, and *G* are similar to *C*.[21]

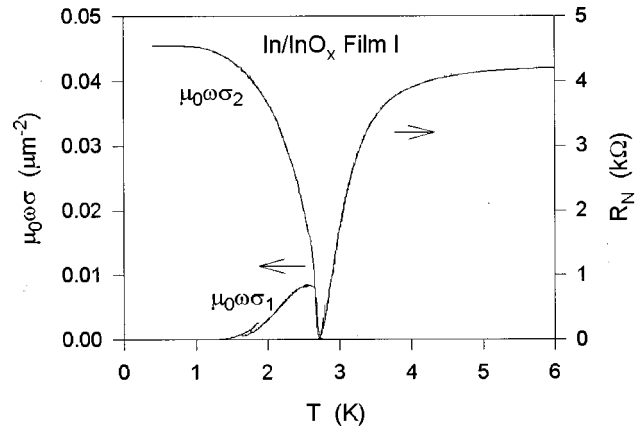

FIG. 4. $\mu_0\omega\sigma$ measured at 50 kHz and the normal state sheet resistance for In/InO$_x$ film *I*. The uncertainty in both R_N and $\mu_0\omega\sigma_2$ is about 10%.

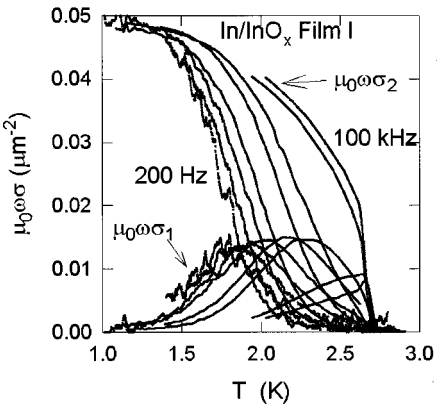

FIG. 5. T dependence of $\mu_0\omega\sigma$ for In/InO$_x$ film *I* at $f=0.2$, 0.5, 1, 2, 5, 10, 50, and 100 kHz. $\mu_0\omega\sigma_2$ increases monotonically with frequency near the transition, and $\mu_0\omega\sigma_1$ peaks at higher temperatures as frequency is increased.

Similar results are found for In/InO$_x$ film *I*. Figure 4 shows $\mu_0\omega\sigma_1$ and $\mu_0\omega\sigma_2$ at 50 kHz and the normal-state resistance, $R_N(T)$. $R_N\rightarrow 0$ at the same temperature that superfluid appears, indicative of an electrically homogeneous film, even though the microstructure is an amorphous composite. Figure 5 shows $\mu_0\omega\sigma(\omega,T)$ and Fig. 6 shows $R(\omega,T)$ and $L^{-1}(\omega,T)$ for 200 Hz$\leqslant f\leqslant$100 kHz. The important qualitative features are the same as for MoGe films.

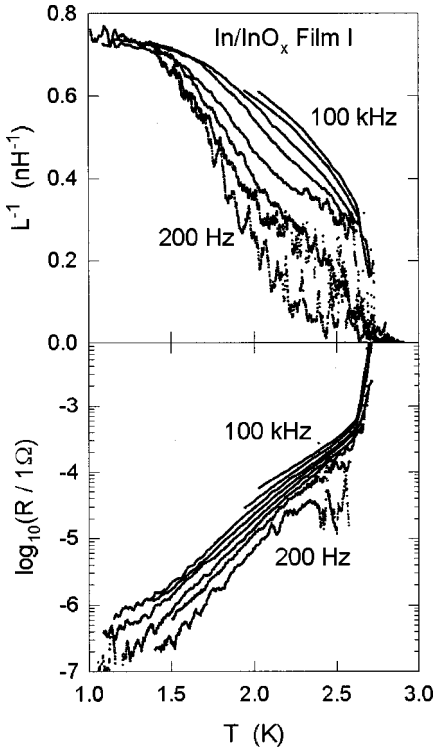

FIG. 6. T dependencies of L^{-1} and R for In/InO$_x$ film *I*, calculated from data in Fig. 5.

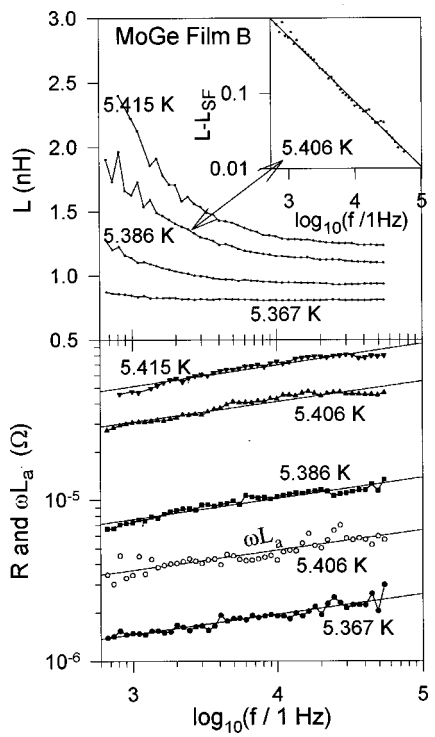

FIG. 7. Top panel shows L vs f for four temperatures. The inset shows that $L_a = L - L_{SF} \propto \omega^{-0.875}$. The bottom panel shows R (filled symbols) for the same 4 temperatures as well as ωL_a for one temperature (open circles). All five of these impedances are proportional to $\omega^{0.13 \pm 0.02}$.

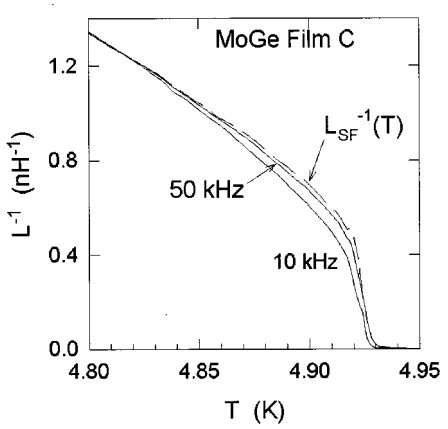

FIG. 8. Example of the extrapolation procedure used to obtain $L_{SF}^{-1}(T)$ for film C. The solid lines are measurements at $f = 10$ and 50 kHz. The dashed line is the extrapolation to high frequency, which is L_{SF}^{-1}.

At 50 kHz, R begins to increase rapidly at the same temperature ($T_C \approx 2.685$ K) where L^{-1} begins to drop, and there is an anomalous impedance below T_C that is frequency dependent down to at least 200 Hz. We note that Ref. 12 found a similar frequency dependence for L^{-1} in an In/InO$_x$ film. They did not present data for R. A minor quantitative difference between In/InO$_x$ and a-MoGe is that for In/InO$_x$, $R(\omega, T)$ increases with T with an activation energy of about $2.2U_0(T)$.

The frequency dependence of the anomalous impedance is weak and extends to remarkably low frequencies. To explore frequency dependence in detail, measurements were made at fixed T for MoGe film B while sweeping the frequency. Noise at low ω was reduced by averaging thousands of measurements over periods of about 10 min. Figure 7 shows results at four temperatures. The top panel shows that L decreases and approaches a constant as ω increases. The inset of the top panel shows a fit of $\log(L - L_{SF})$ to const $+(b-1)\log(f)$, where L_{SF} was adjusted to obtain the best straight line. The best fit has $b = 0.125$, so the anomalous reactance is $\omega L_a = A(T)\omega^{0.125}$. The bottom panel in Fig. 7 shows R vs f (solid symbols) at four temperatures, and ωL_a vs f at $T = 5.406$ K (open circles). For all temperatures, R and ωL_a are proportional to ω^b, with $b = 0.13 \pm 0.02$. For In/InO$_x$ film I, $b \approx 0.20 \pm 0.05$. Our main point is that $Z_a(\omega, T) = R + \omega L_a$ is a weak function of ω at surprisingly low frequencies.

We interpret $L_{SF}(T)$ as the expected superfluid inductance, including vortex-antivortex pairs. Figure 8 illustrates that L_{SF}^{-1} is not much larger than the measured L^{-1} at the highest experimental frequency, typically 50 or 100 kHz. The lower curves are $L^{-1}(T)$ measured at 10 kHz and 50 kHz, and the dashed curve is $L_{SF}^{-1}(T)$ which has been calculated from the 10 kHz and 50 kHz data sets and the assumption that $\omega L_a = A(T)\omega^{0.14}$. For $T < T_C$, the dashed curve is quite close to the 50 kHz data, so errors in extrapolation are small.

IV. EXPECTED BEHAVIOR OF VORTEX-ANTIVORTEX PAIRS

In this section, we construct a simple model of vortex-antivortex pairs coexisting with a background superfluid agitated by nonvortex thermal phase fluctuations. The model provides estimates for various important parameters such as the density of vortices at the unbinding transition, the width of the critical region, and the contribution of vortex-antivortex pairs to the sheet impedance below the critical region. It supports our conclusions that the unbinding transition for conventional vortex-antivortex pairs occurs as expected, and that there is an anomalous dissipative mechanism that cannot be described with conventional vortex-antivortex pairs. Since interactions among pairs are important only in a very narrow region near the unbinding transition,[22] and our main focus lies below this region, we will neglect interpair interactions. Our estimations for vortex-pair properties are more accurate if we calculate the characteristic superconducting energy introduced in Eq. (1) by replacing the mean-field sheet inductance with the inductance of the background superfluid, which is suppressed by nonvortex thermal phase fluctuations, but is smooth through the pair-unbinding transition. We denote this energy as U_0.

To begin, we review how fluctuation effects evolve with increasing temperature. At a low temperature, say, $k_B T/U_0(T) \approx 1/20$, small amplitude, non-vortex phase fluctuations suppress the background superfluid density, $n_{S,B}(T)$, below the mean-field density, $n_{S0}(T)$, by perhaps a

percent,[23] and the areal density, $n_p(T)$, of vortex pairs is negligible. As T increases, nonvortex phase fluctuations increase in intensity, ultimately suppressing $n_{S,B}(T)$ to 70–75 % of $n_{S0}(T)$ at the unbinding transition. These background phase fluctuations are an essential part of the story because they are responsible both for generating vortex-antivortex pairs and for driving their Brownian motion. They are considered in some detail in Ref. 24. For reference, since $n_{S,B}(T) \approx 0.75 n_{S0}(T)$ at the unbinding transition, KTB theory predicts a transition at $k_B T/U_0(T) \approx 0.75\pi/2 \approx 1.2$.

To estimate the density of vortex-antivortex pair excitations, we need their energy relative to the Meissner state. The calculation is straightforward. The energy has three portions: (1) E_M, associated with suppression of, and gradients in, the magnitude of the order parameter; (2) E_K, the kinetic energy of supercurrents, and (3) magnetic field energy, which is negligible. E_M is given by[25,26]

$$E_M = (\pi U_0/2) \int_0^\infty dr\, r[(1-g^2)^2 + 2(\nabla g)^2], \qquad (2)$$

where $g(r)$ is the normalized order parameter and r is the distance from the center of the vortex divided by the coherence length, ξ. For a single vortex in the high κ limit, $E_M = 2.45U_0$. (Ref. 27 used half of this value.) The energy E_K is calculated from the sheet supercurrent density, $K_S(r)$:

$$E_K = \pi \mu_0 \lambda_\perp \int_0^\infty dr\, r g^2(r) K_S^2(r), \qquad (3)$$

where $\lambda_\perp \equiv \lambda^2/d$ and λ is the magnetic penetration depth. Within the London model for a single vortex, the sheet supercurrent density $K_S(r)$ outside the core is proportional to $1/r$ for $\xi \ll r \ll \lambda_\perp$, and proportional to $1/r^2$ for $r \gg \lambda_\perp$.[28] To get $K_S(r)$ and $g(r)$ in the core of a single vortex, we solved the GL differential equation numerically as has been done previously.[25]

To calculate the energy of a vortex and antivortex separated by a distance ρ, one should solve the GL differential equations, but this has not been accomplished since the azimuthal symmetry of one vortex is broken for a pair. E_M for a vortex-antivortex pair is approximately twice E_M for a single vortex. To determine E_K for a vortex-antivortex pair, we integrated the kinetic energy density of the supercurrents associated with a pair,[21] assuming that the suppercurrent patterns for a single vortex could be added. Figure 9 shows the calculated energy of a pair as a function of ρ. To a good approximation, $E_{\rm pair}$ increases logarithmically with ρ:[4,5]

$$E_{\rm pair}(\rho) = E_{C,\rm pair}(\rho_0) + 2\pi U_0 \ln(\rho/\rho_0), \qquad (4)$$

where ρ_0 is the size of the smallest pair that is well defined. We take $\rho_0 = 2\xi(T)$. Figure 9 shows that Eq. (4) is a very good approximation for $\rho > 3\xi$. Pairs smaller than 2ξ are effectively fluctuations in the order parameter amplitude, since there is very little current associated with them. Given that the energy of minimum sized pairs is uncertain we take $E_{C,\rm pair}(\rho_0)$ to be the value of the logarithmic asymptote (dashed line in Fig. 9) evaluated at ρ_0. This yields

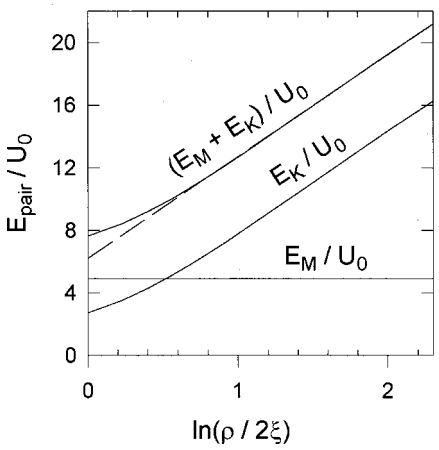

FIG. 9. Calculated energy of a vortex-antivortex pair in a high κ ($\kappa \equiv \lambda/\xi$), 2D superconductor. E_M is the energy from suppression and gradients of the magnitude of the order parameter, E_K is the kinetic energy of the supercurrents associated with the pair. The dashed line is the logarithmic asymptote of the pair energy, and its value at $\rho = 2\xi$ yields a core energy of $6.22U_0$ for a pair of minimum size, $\rho_0 = 2\xi$.

$E_{C,\rm pair}(2\xi) = 6.22U_0$. This procedure gives the correct energy for pairs larger than about 4ξ and much smaller than $\lambda_\perp$, which is the range of interest here.

The density of vortex pairs, $n_p(T)$, can be estimated by assuming that all pairs are of the minimum size, ρ_0, and calculating the probability of finding a pair in each $2\rho_0 \times 2\rho_0$ cell of the film:

$$n_p = [1/4\rho_0^2] N_0 e^{-E_{C,\rm pair}(\rho_0)/k_B T} / [1 + N_0 e^{-E_{C,\rm pair}(\rho_0)/k_B T}], \qquad (5)$$

where N_0 is the number of independent ways that the pair can be oriented in the cell. Roughly, the vortex can be in any quadrant of the cell, and the antivortex can be in any of the other three quadrants, so $N_0 \approx 12$. Certainly, N_0 should be larger than unity. Our conclusions are insensitive to its precise value. The fraction, f_N, of the film area that is ''normal'' is approximately the fraction occupied by vortex cores: $f_N \approx n_p 4\xi^2$. We would expect f_N to be roughly one percent at the transition; certainly it must be much less than the 2D percolation value of 50%, and to decrease very rapidly below the transition. Consistent with this expectation, from Eq. (5) we estimate $f_N = 0.001$ at $k_B T/U_0 \approx 0.7$, and $f_N = 0.01$ at $k_B T/U_0 \approx 1$ with parameters, $\rho_0 = 2\xi$, $E_{C,\rm pair} = 6U_0$ and $N_0 = 12$. Thus, just above the unbinding transition, where all pairs are unbound and resistive, we expect the sheet resistance to be a few percent of R_N, a reasonable value.[7] We will combine Eq. (5) with the estimated impedance of individual vortex pairs to compare to the measured sheet impedance.

We now estimate the upper limit of the critical region and the pair unbinding transition temperature. The upper limit of the critical region is the temperature where the rms size of noninteracting pairs diverges. The probability that a pair has a separation $\rho > \rho_0$ is determined by the increase in free energy with separation, $(2\pi U_0 - k_B T)\ln(\rho/\rho_0)$, which leads to an rms pair size[1]

$$\langle\rho^2\rangle^{1/2}/\rho_0=[\pi U_0/k_BT-1]^{1/2}/[\pi U_0/k_BT-2]^{1/2}, \quad (6)$$

that diverges at $k_BT/U_0(T)=\pi/2$. Vortex pair unbinding occurs at a slightly lower temperature, where pairs overlap so much that it is impossible to say which vortex is paired with which antivortex. If we take the criterion to be $[n_p\langle\rho^2\rangle]^{1/2}\approx 0.4$, then with $N_0=12$ and $E_{C,\mathrm{pair}}=6U_0$, unbinding occurs at $k_BT/U_0(T)\approx 1.3$. As noted above, KTB theory finds an unbinding transition at $k_BT/U_0(T)\approx 1.2$, very close to our simple estimate. Evidently details are not important. The critical region above the unbinding transition occupies temperatures, $1.2<k_BT/U_0(T)<\pi/2$. Since $U_0\approx 0.75U_{00}$ near T_C, then for our films the critical region extends approximately one-third of the way from T_C to T_{C0}.

A typical experimental resistance at the upper edge of the critical region is a few tenths of a percent of the normal-state resistance.[7] This suggests that at the transition, vortex cores occupy somewhat less than 1% of the film area. We can incorporate this important observation into the model by letting N_0 in Eq. (5) be closer to 3 than to 12. Thus, the model is consistent with the measured unbinding temperature and resistance above the critical region.

Let us now consider the inductance of vortex pairs below the critical region. In JJ arrays vortex-pair and nonvortex fluctuations together suppress the inverse inductance to about 60% of its mean-field value just below the unbinding transition. If nonvortex fluctuations suppress the inverse inductance of the background superfluid to 75% of its mean-field value, then the additional inductance of vortex-antivortex pairs is about 25% of the measured inductance. Our simple model is consistent with this result. To estimate the vortex-pair inductance, first, we note that a typical vortex-antivortex pair is small. The probability, $P(\rho)$, that a given pair has a separation greater than ρ is

$$P(\rho)=(\rho_0/\rho)^{2\pi U_0/k_BT-2}. \quad (7)$$

Thus, at $k_BT/U_0=1$, i.e., only slightly below the unbinding transition, the probability for a pair to be ten times larger than its minimum size, i.e., $\langle\rho^2\rangle^{1/2}/\rho_0=10$, is already about 10^{-4}. The probability of unbound pairs, with $\langle\rho^2\rangle^{1/2}\approx\lambda_\perp\approx 1000\rho_0$, is less than 10^{-12} and therefore negligible for $k_BT/U_0<1$.

We estimate the impedance of a bound pair as follows. A pair with separation ρ has a dipole moment, $\rho\phi_0$, and polarizes in response to the average background supercurrent, $\mathbf{K}_s$, (taken to be along the x direction and sinusoidal in time). The impedances of the background superfluid and vortex pairs are in series as long as the pairs are not too close together, which is the simplified case under consideration here. The ac supercurrent requires an average electric field, $E_{s,x}=-i\omega L_sK_{s,x}$, where L_s is the inductance of the superfluid. In thermal equilibrium, each dipole has an average y component: $[(\rho\phi_0)^2/k_BT]K_s$. The net polarization, $P_y(\omega)$, is proportional to $K_{s,x}$, hence to $E_{s,x}(\omega)/i\omega$:

$$P_y(\omega)=\chi_p(\omega)E_{s,x}(\omega)/-i\omega, \quad (8)$$

where the low-frequency susceptibility, χ_p, is

$$\chi_p=n_p\langle\rho^2\rangle\phi_0^2/[L_sk_BT(1-i\omega\tau)]. \quad (9)$$

τ, an average equilibration time that depends on $\langle\rho^2\rangle^{1/2}$, is estimated below. The average electric field due to polarizing pairs arises from their velocity along y

$$E_{p,x}=-i\omega P_y(\omega)=\chi_pE_{s,x}, \quad (10)$$

so the sheet impedance of background superfluid and vortex pairs is

$$Z(\omega,T)=E_{s,x}(1+\chi_p)/K_{s,x}=-i\omega L_s\varepsilon_p, \quad (11)$$

where the real and imaginary parts of the inverse vortex pair dielectric function, ε_p^{-1}, are related by Kramers-Kronig transform.[5] The pair impedance,

$$Z_p=R_p(\omega,T)+i\omega L_p(T)\equiv E_{p,x}/K_{s,x}$$
$$\approx i\omega n_p\langle\rho^2\rangle\phi_0^2/k_BT(1-i\omega\tau), \quad (12)$$

is inductive at $\omega\ll 1/\tau$ and resistive for $\omega\gg 1/\tau$.

τ is the time for a typical vortex-antivortex pair to sample all possible orientations relative to $\mathbf{K}_S$, i.e., $1/\tau\approx D/\langle\rho^2\rangle$, where D is the vortex diffusion constant. With the expression, $D=28e^2\xi^2k_BTR_N/\hbar^2\pi=(7\xi^2/\pi)(k_BT/\hbar)(R_N/R_Q)$,[3,4] with $R_Q\equiv\hbar/4e^2\approx 1\,\mathrm{k}\Omega$, and $\langle\rho^2\rangle^{1/2}\approx 2\xi$, we have

$$1/\tau=(7/4\pi)(k_BT/\hbar)(R_N/R_Q). \quad (13)$$

With typical values, $R_N=300\,\Omega$ and $T=5$ K, we find $1/\tau\approx 10^{11}$ rad/s, which is five orders of magnitude larger than our maximum experimental ω, 6×10^5 rad/s, so vortex pairs are expected to be inductive below T_C, regardless of the simplicity of the model.

For film C, $k_BT/U_0(T)\approx 1.0$ at 4.903 K, and $L_{\mathrm{SF}}(4.903\,\mathrm{K})$ is about 1.2 nH, so the contribution of vortex pairs should be about 0.3 nH. From Eq. (12) and $n_p\langle\rho^2\rangle\approx 0.01$, the estimated inductance of vortex pairs is about 0.6 nH. Of course, $n_p\langle\rho^2\rangle$ may be an order of magnitude smaller than 0.01, and the estimated inductance of pairs would then be near 0.06 nH. Given the uncertainties, we consider this to be good agreement and further confirmation that the observed drop in L_{SF}^{-1} represents the unbinding of a low density of conventional vortex-antivortex pairs. Figure 10 shows that the drop in L_{SF}^{-1} is consistent with the universal prediction of KTB theory.

Finally, we show that the resistance of vortex pairs should be much smaller than what we observe. Motion of pairs subject to an ac supercurrent would cause dissipation due to viscosity, and give rise to a small resistance, R_p. From Eqs. (12) and (13)

$$R_p/\omega L_p=(4\pi/7)(\hbar\omega/k_BT)R_Q/R_N. \quad (14)$$

Clearly the quadratic frequency dependence predicted for R_p is stronger than is observed for R below the unbinding transition. For a quantitative comparison, we need to pick a particular frequency, arbitrarily taken to be 50 kHz. For film C, Eq. (14) yields $R_p/\omega L_p\approx 10^{-6}$. If we take $L_p=0.3$ nH, then R_p should be about $10^{-10}\,\Omega$, which is six orders of magnitude smaller than the measured sheet resistance just below the transition. Thus the dissipation of conventional pairs is

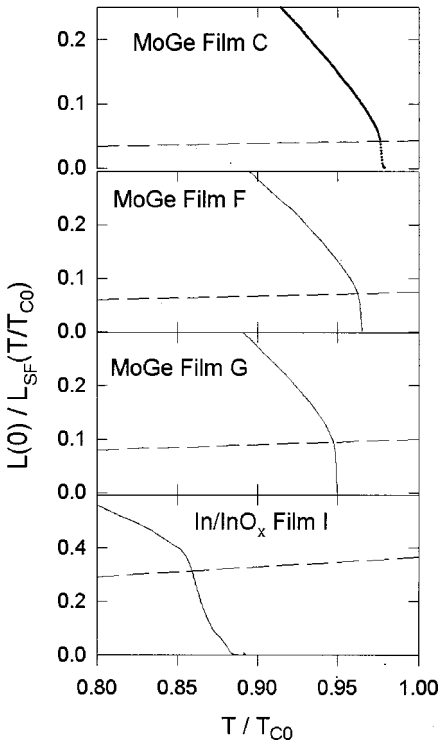

FIG. 10. $L_{SF}(0)/L_{SF}(T/T_{C0})$ vs T/T_{C0} for four films. The intersection of dashed line and data is where the KTB vortex-pair unbinding transition is predicted to occur. As normal-state sheet resistance increases (top to bottom), the transition occurs further below the mean-field transition temperature, T_{C0}, and at a higher fraction of the $T=0$ inverse sheet inductance.

undetectable at our measurement frequencies. The anomalous impedance below T_C remains to be explained.

V. DISCUSSION OF $Z_a(\omega,T)$

Experimentally, the anomalous sheet impedances, $Z_a(\omega,T)=R(\omega,T)+i\omega L_a(\omega,T)$, of a-MoGe and In/InO$_x$ films are quite similar in their most important features: (1) Over the experimental frequency range, 100 Hz to 100 kHz, Z_a has a weak dependence on ω, being roughly proportional to ω to a small T-independent power; (2) consistent with the weak frequency dependence, Z_a is mostly resistive: $R/\omega L_a \approx 8$, independent of ω and T; (3) Z_a has an Arrhenius T dependence, with an excitation energy of about $3.5U_0$ in a-MoGe and $2.2U_0$ for In/InO$_x$. These similarities argue that the observed behavior is generic to 2D superconductors, and not due to microstructure.

Since the anomalous impedance is dissipative, it involves vortices and antivortices in some configuration. The Arrhenius T dependence of $Z_a(\omega,T)$ suggests that the dissipative excitations are not interacting, so the frequency dependence is intrinsic to each excitation and not a result of critical behavior. The frequency dependence is the most puzzling feature because it persists below the conventional unbinding transition, and to such low frequencies. On the first point, we note that we were able to measure a nonzero sheet resistance down to $k_BT/U_0(T)\approx 1/3$, well below the conventional transition at $k_BT/U_0(T)\approx 1.2$. When Pierson *et al.*[11] reanalyzed the I-V data of van der Zant *et al.*[29] on a Josephson junction array, allowing the dynamical exponent z to be a free parameter, they found that the transition occurred at $k_BT/U_0(T) \approx 0.5$, also well below the conventional transition. Our experiment would require data at lower frequencies and temperatures to determine whether there is an S-N transition below the unbinding temperature.

On the second point, we note that the excitation energy of about $3.5U_0$ suggests that the anomalous excitation has spatial dimensions of a single vortex, a few coherence lengths. Characteristic times associated with this distance are much shorter than the experimental time scale of 10 ms. The time for an electron or phonon to travel a coherence length ballistically is very short. Vortex diffusion sets a time scale of $\hbar/k_BT$ for typical films, which is very short. Another characteristic vortex time is the time for a vortex-antivortex pair to annihilate, in the absence of Brownian perturbations. This time is proportional to the square of their initial separation, $\rho(0)$: $\tau_{\text{annih}}\approx(L_{SF}/R_N)[\rho(0)/\xi(T)]^2$, which is about equal to $\hbar/k_BT_C$ for our films, and is too short to account for frequency dependence at 100 Hz.

Other experiments have observed similar anomalous low-frequency behavior in films: Fiory *et al.*[12] down to 14 Hz in an In/InO$_x$ film similar to ours, and Festin *et al.*[30] down to 0.1 Hz in a YBCO film. The phenomenon is not confined to continuous films. In a triangular Josephson junction array at $k_BT/U_0\approx 1/2$ ($T=3.27$ K; $T_C\approx 3.70$ K; $R_N/L \approx 3\times 10^6$ rad/s). Theron *et al.*[15] observed a 40% increase in sheet inductance (0.7 to 1 nH) as frequency decreased from 10 to 0.16 kHz. For comparison, in film C at $k_BT/U_0 \approx 1/2$ ($T=4.83$ K; $T_C=4.92$ K; $R_N/L\approx 3\times 10^{11}$ rad/s), we observed an increase of 70% (0.9 to 1.5 nH) as frequency decreased from 10 kHz to 0.19 kHz. The quantitative similarity is striking, considering the physical differences between films and arrays. Theron *et al.* concluded that the diffusion of field-induced vortices in their arrays was anomalously sluggish.

It has been suggested that the anomalous excitation might be single thermally excited vortices created at the edges of the films.[32] We do not have a model for the dynamics of these vortices, so further measurements would be needed to assess their contribution to the measured sheet impedance.

VI. CONCLUSION

The sheet impedances of 2D superconducting a-MoGe and In/InO$_x$ films exhibit features expected from the presence of thermally excited vortex-antivortex pairs, especially, rapid increases in resistance and inductance at the same temperature due to pair unbinding. In addition, below the unbinding transition, there exists an anomalous, dissipative excitation with dynamics that extend to frequencies well below

characteristic frequencies for vortex pairs. The anomalous excitation seems to exist in arrays of Josephson junctions, as well as films. Its Arrhenius T dependence suggests that slow dynamics are a property of individual excitations rather than arising from interactions among conventional vortex-antivortex pairs. Identifying this excitation remains as an important challenge to the community. Understanding this excitation will improve our insight into the $T=0$ superconductor-to-insulator transition and bolster confidence in our ability to interpret the sheet impedance of cuprate superconductors.

ACKNOWLEDGMENTS

This work was supported in part by U.S. DOE Grant No. DE-FG02-90ER45427 through the Midwest Superconductivity Consortium. J.M.G. gratefully acknowledges research support from the NHMFL In-House Research Program, under NSF/DMR Contract No. 9527035 and S.J.T. gratefully acknowledges support from Ohio State University and technical assistance from Margarita Rokhlin and Dr. Saad Hebboul.

*Present address: Pennsylvania State Univ. Graduate Program in Acoustics, P. O. Box 30, State College, PA 16804-8783.

†Present address: Bell Laboratories, Lucent Technologies, 600-700 Mountain Avenue, Murray Hill, NJ 07974.

[1] J. M. Kosterlitz and D. J. Thouless, J. Phys. C **6**, 1181 (1973).

[2] V. L. Berezinskii, Zh. Eksp. Teor. Fiz. **61**, 1144 (1971) [Sov. Phys. JETP **34**, 610 (1972)].

[3] V. Ambegaokar, B. I. Halperin, D. R. Nelson, and E. D. Siggia, Phys. Rev. Lett. **40**, 783 (1978); Phys. Rev. B **21**, 1806 (1980); V. Ambegaokar and S. Teitel, *ibid.* **19**, 1557 (1979).

[4] B. I. Halperin and D. R. Nelson, J. Low Temp. Phys. **36**, 599 (1979).

[5] P. Minnhagen, Rev. Mod. Phys. **59**, 1001 (1987).

[6] A. F. Hebard and A. T. Fiory, Phys. Rev. Lett. **44**, 291 (1980).

[7] K. Epstein, A. M. Goldman, and A. M. Kadin, Phys. Rev. Lett. **47**, 534 (1981).

[8] A. M. Kadin, K. Epstein, and A. M. Goldman, Phys. Rev. B **27**, 6691 (1983).

[9] J. M. Repaci, C. Kwon, T. Venkatesan, Qi Li, X. Jiang, R. E. Glover III, C. J. Lobb, and R. S. Newrock, Phys. Rev. B **54**, R9674 (1996).

[10] S. T. Herbert *et al.*, Phys. Rev. B **57**, 1154 (1998).

[11] S. W. Pierson, M. Friesen, S. M. Ammirata, J. C. Hunnicutt, and L. A. Gorham, Phys. Rev. B **60**, 1309 (1999).

[12] A. T. Fiory, A. F. Hebard, and W. I. Glaberson, Phys. Rev. B **28**, 5075 (1983).

[13] A. Yazdani, Ph.D. thesis, Stanford University, 1994.

[14] B. Jeanneret, Ph. Fluckiger, J. L. Gavilano, Ch. Leeman, and P. Martinoli, Phys. Rev. B **40**, 11 374 (1989).

[15] R. Theron, J.-B. Simond, Ch. Leemann, H. Beck, P. Martinoli, and P. Minnhagen, Phys. Rev. Lett. **71**, 1246 (1993).

[16] Ch. Leeman, Ph. Lerch, G.-A Racine, and P. Martinoli, Phys. Rev. Lett. **56**, 1291 (1986).

[17] W. Shih and D. Stroud, Phys. Rev. B **32**, 158 (1985) and references therein. These authors find for triangular, square, and honeycomb lattices, respectively, $k_BT_C/U_{00}(T_C)=0.87$, 0.91, and 1.00, and $L_0(T_C)/L(T_C)=0.53$, 0.59, and 0.64.

[18] S. J. Turneaure, T. R. Lemberger, and J. M. Graybeal, Phys. Rev. Lett. **84**, 987 (2000).

[19] J. R. Clem and M. W. Coffey, Phys. Rev. B **46**, 14 662 (1992).

[20] S. J. Turneaure, E. R. Ulm, and T. R. Lemberger, J. Appl. Phys. **79**, 4221 (1996); S. J. Turneaure, A. A. Pesetski, and T. R. Lemberger, *ibid.* **83**, 4334 (1998).

[21] S. J. Turneaure, Ph.D. thesis, Ohio State University, 1999.

[22] L. C. Davis, M. R. Beasley, and D. J. Scalapino, Phys. Rev. B **42**, 99 (1990).

[23] Classically, nonvortex phase fluctuations suppress the effective superfluid density of a Josephson junction array by a factor of $1-k_BT/4U_{00}(T)$ at low T, which extrapolates to 0.75 at T_C. Calculations (Ref. 17) show that the additional effect of vortex-antivortex pairs becomes comparable only very close to the unbinding transition, i.e., for $k_BT/U_0(T)>0.7$, where the transition is at $k_BT/U_0(T)=0.9$.

[24] T. R. Lemberger, A. A. Pesetski, and S. J. Turneaure, Phys. Rev. B **61**, 1483 (2000).

[25] P. Minnhagen and M. Nylen, Phys. Rev. B **31**, 5768 (1985).

[26] C.-R. Hu, Phys. Rev. B **6**, 1756 (1972).

[27] M. Gabay and A. Kapitulnik, Phys. Rev. Lett. **71**, 2138 (1993).

[28] J. Pearl, Appl. Phys. Lett. **5**, 65 (1964); *Low-Temp. Phys.-LT9*, edited by M. Yaqub and J. G. Daunt (Plenum, New York, 1965), pp. 437–453.

[29] H. S. J. van der Zant, H. A. Zant, H. A. Rijken, and J. E. Mooij, J. Low Temp. Phys. **79**, 289 (1990).

[30] O. Festin, P. Svedlindh, B. J. Kim, P. Minnhagen, R. Chakalov, and Z. Ivanov, cond-mat/9910519 (unpublished).

[31] J. M. Graybeal, Physica B **135**, 113 (1985).

[32] S.-I. Lee (private communication).